Molecular Cell
Short Article

A Genome-wide RNA Interference Screen Reveals that Variant Histones Are Necessary for Replication-Dependent Histone Pre-mRNA Processing

Eric J. Wagner,[1,5] Brandon D. Burch,[2,5] Ashley C. Godfrey,[3] Harmony R. Salzler,[2] Robert J. Duronio,[2,3,4,*] and William F. Marzluff[1,2,3,4,*]
[1]Department of Biochemistry and Biophysics
[2]Curriculum in Genetics and Molecular Biology
[3]Department of Biology
[4]Program in Molecular Biology and Biotechnology
University of North Carolina at Chapel Hill, Chapel Hill, NC 27599, USA
[5]These authors contributed equally to this work.
*Correspondence: duronio@med.unc.edu (R.J.D.), marzluff@med.unc.edu (W.F.M.)
DOI 10.1016/j.molcel.2007.10.009

SUMMARY

Metazoan replication-dependent histone mRNAs are not polyadenylated and instead end in a conserved stem loop that is the *cis* element responsible for coordinate posttranscriptional regulation of these mRNAs. Using biochemical approaches, only a limited number of factors required for cleavage of histone pre-mRNA have been identified. We therefore performed a genome-wide RNA interference screen in *Drosophila* cells using a GFP reporter that is expressed only when histone pre-mRNA processing is disrupted. Four of the 24 genes identified encode proteins also necessary for cleavage/polyadenylation, indicating mechanistic conservation in formation of different mRNA 3′ ends. We also unexpectedly identified the histone variants H2Av and H3.3A/B. In *H2Av* mutant cells, U7 snRNP remains active but fails to accumulate at the histone locus, suggesting there is a regulatory pathway that coordinates the production of variant and canonical histones that acts via localization of essential histone pre-mRNA processing factors.

INTRODUCTION

Metazoan histone pre-mRNAs lack introns and require only a single 3′ end processing event to form mature mRNA, which terminates in an evolutionarily conserved stem loop (SL) rather than a poly(A) tail. Processing occurs by endonucleolytic cleavage downstream of the SL and 5′ of a purine-rich sequence, the histone downstream element (HDE) (Figure 1A). Cleavage requires a protein that binds the SL (the stem loop binding protein or SLBP) (Wang et al., 1996), and U7 snRNP, which interacts with the HDE via base-pairing with U7 snRNA (Mowry and Steitz, 1987). The 3′ SL remains bound by SLBP and is necessary for the export, translation, and eventual decay of histone mRNA. Thus, accurate pre-mRNA processing is essential for the expression of histones during S phase.

A number of histone pre-mRNA processing factors have been identified from mammals, *Drosophila*, and *Xenopus*, including SLBP, U7 snRNA, and U7 snRNP-specific components Lsm11, Lsm10, and ZFP100 (Dominski et al., 2002; Pillai et al., 2001, 2003). Recent in vitro experiments have unexpectedly found that factors involved in the canonical cleavage/polyadenylation reaction, such as CPSF73 and Symplekin, also participate in histone pre-mRNA processing (Dominski et al., 2005; Kolev and Steitz, 2005). However, it is unclear whether all or only a subset of the cleavage/polyadenylation factors are necessary for processing histone pre-mRNAs. To address this and to identify additional factors necessary for histone pre-mRNA processing in intact cells, we carried out a genome-wide RNA interference screen in cultured *Drosophila* cells to identify proteins necessary for production of histone mRNA.

RESULTS AND DISCUSSION

To facilitate screening, we developed a visual assay for histone pre-mRNA processing. The assay is based on our observation that mutation of either the *Slbp* or *U7* snRNA genes in *Drosophila* results in expression of incorrectly processed histone mRNAs (Godfrey et al., 2006; Sullivan et al., 2001). These misprocessed mRNAs are polyadenylated due to transcriptional readthrough and subsequent usage of canonical poly(A) signals downstream of the HDE. We postulated that readthrough to a downstream polyadenylation site would be a general phenotype associated with reduced expression of any factor required for histone pre-mRNA processing, and we designed a minigene capable of reporting histone pre-mRNA misprocessing. The minigene reporter contains a GFP

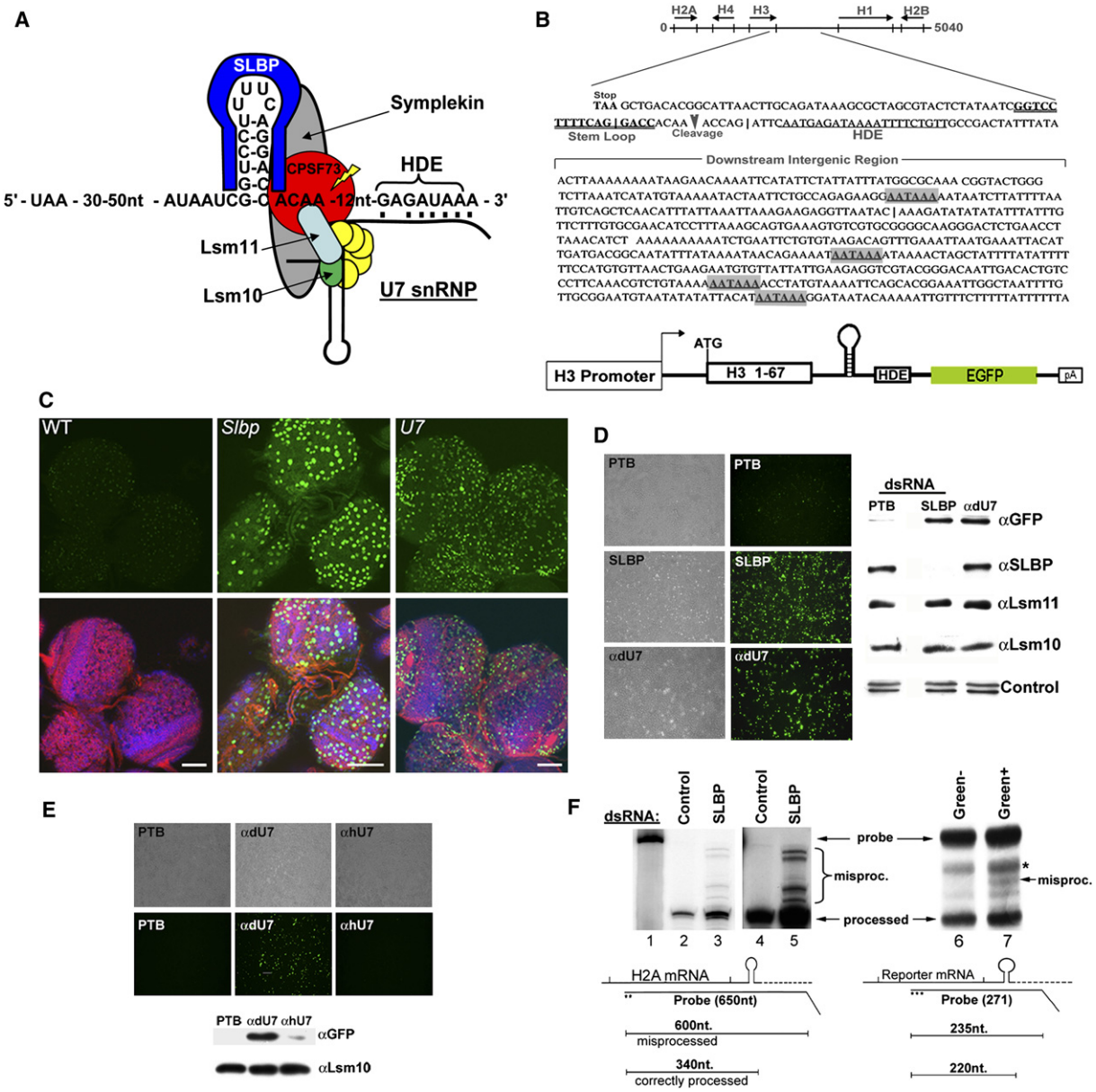

Figure 1. A Reporter for *Drosophila* Histone Pre-mRNA Processing

(A) Schematic of *Drosophila* histone pre-mRNA processing machinery.

(B) Diagram of *Drosophila* histone gene cluster showing the H3-H1 intergenic region containing the cryptic cleavage and polyadenylation sites (gray boxes) (Lanzotti et al., 2002), and a schematic of the reporter.

(C) Confocal images of third instar larval brains containing the transgenic reporter and stained with anti-GFP (green), anti-phosphotyrosine (for cell cortex labeling; red), and DAPI (blue). Scale bar, 50 μm.

(D) Left, brightfield (left) and fluorescence images (right) of Dmel-2 cells treated with dsRNA to PTB (control) or SLBP or with the αU7 oligonucleotide. Right, corresponding western blot analysis.

(E) Bright field and fluorescence images and corresponding western blot analysis of cells treated with PTB dsRNA or a 2′O-CH_3 oligonucleotide targeting *Drosophila* or human U7 snRNA.

(F) S1 nuclease protection assay (schematic at bottom) of endogenous H2A mRNA (lanes 2–5) or the reporter mRNA (lanes 6 and 7) isolated from Dmel-2 cells treated with PTB dsRNA (lanes 2, 4, and 6) or a dsRNA that activated readthrough (lanes 3, 5, and 7). Note that lanes 4 and 5 are a darker exposure of lanes 2 and 3. Lane 1 contains input probe.

ORF and poly(A) site downstream of the SL and HDE of the histone H3 gene (Figure 1B and see Figure S1 in the Supplemental Data available with this article online). Normal histone pre-mRNA processing results in mRNA lacking the GFP ORF, while misprocessing leads to readthrough transcription and production of mRNA encoding GFP.

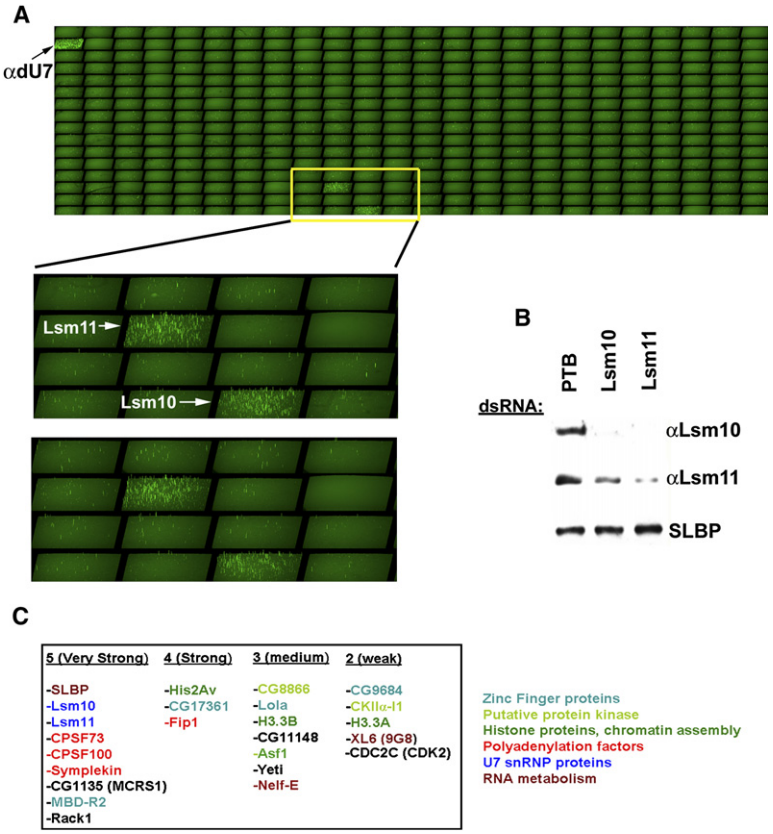

Figure 2. Results of the Screen

(A) Fluorescence images of Dmel-2 cells grown on plate 18 of dsRNA library and transfected with reporter. Cells in column 1, row 2 were treated with αU7 oligonucleotide. The inset is a higher magnification view of 16 wells, two of which contain dsRNA for Lsm10 or Lsm11, from replicate experiments.

(B) Western blot analysis of lysates from Dmel-2 cells treated with dsRNA targeting PTB (control), Lsm10, or Lsm11.

(C) Table of hits from the genome-wide screen categorized numerically by qualitative strength of reporter signal and by color for relevant domains or putative/known functions.

Transgenic flies containing the reporter display robust GFP expression in *U7* snRNA or *Slbp* null mutant brains compared to wild-type controls (Figure 1C). Thus, the reporter recapitulates the requirements for endogenous histone mRNA biosynthesis.

Transfection of the reporter into Dmel-2 cells depleted of SLBP using dsRNA, or with U7 snRNA inhibited using a 2′OCH_3 oligonucleotide complementary to the 5′ end of U7 snRNA (αU7), resulted in GFP expression (Figure 1D). Little GFP signal was seen in cells treated with control dsRNA or a 2′OCH_3 oligonucleotide complementary to human U7 snRNA (Figure 1E). GFP expression occurred after SLBP depletion despite only a low amount of transcriptional readthrough of the endogenous histone genes (Figure 1F, lanes 3 and 5; Figure S2) and a modest (10%–20%) readthrough of the reporter gene (Figure 1F, lane 7), underscoring the sensitivity of the reporter to small amounts of misprocessing.

Using this reporter we performed a genome-wide RNAi screen at the *Drosophila* RNAi Screening Center (www.flyrnai.org) (Boutros et al., 2004). Dmel-2 cells were incubated with dsRNA for 3 days, transfected with the reporter, and analyzed by fluorescence microscopy 48 hr later. About 22,000 dsRNAs were tested in duplicate, resulting in 63 collages of 384-well plates. Plate 18 is shown as an example (Figure 2A). The two positive wells (Figure 2A, inset) contained dsRNA targeting the *Drosophila* orthologs of the human Lsm10 and Lsm11 proteins, specific components of the U7 snRNP (Azzouz and Schumperli, 2003). We synthesized these dsRNAs and found they knocked down endogenous Lsm10 and Lsm11 proteins (Figure 2B).

By visual inspection, we initially scored 90 genes as potentially positive. We synthesized dsRNA targeting each gene and assayed them under identical conditions. Of these, 24 were found to score repeatedly above background (Figure 2C; Figure S3). All of these were confirmed with dsRNA targeting a second site of the mRNA (Figure S4). We identified five previously known components of the histone pre-mRNA processing machinery (SLBP, Lsm11, Lsm10, Symplekin, and CPSF73). Among the other 19 genes are two cleavage/polyadenylation factors (CPSF100 and Fip1), four proteins involved in chromatin structure and assembly (H2a.V, H3.3A, H3.3B, and Asf1), four zinc finger proteins (MBD-R2, CG17361, Lola, and CG9684), and four known/putative signaling molecules (RACK1, CG8866, CKIIα-iI, and Cdk2). Many of these proteins (all of which have potential mammalian orthologs) are largely unstudied, except for the mammalian SR protein 9G8, implicated in alternative splicing (Cramer et al., 2001) and histone mRNA nuclear export (Huang et al., 2003); the cyclin-dependent kinase Cdk2, essential for progression through S phase (Knoblich et al., 1994), and NELF-E, a component of the negative transcription elongation factor (Wu et al., 2005). We did not identify proteins required for U7 snRNP biosynthesis, such as SMN, snRNA

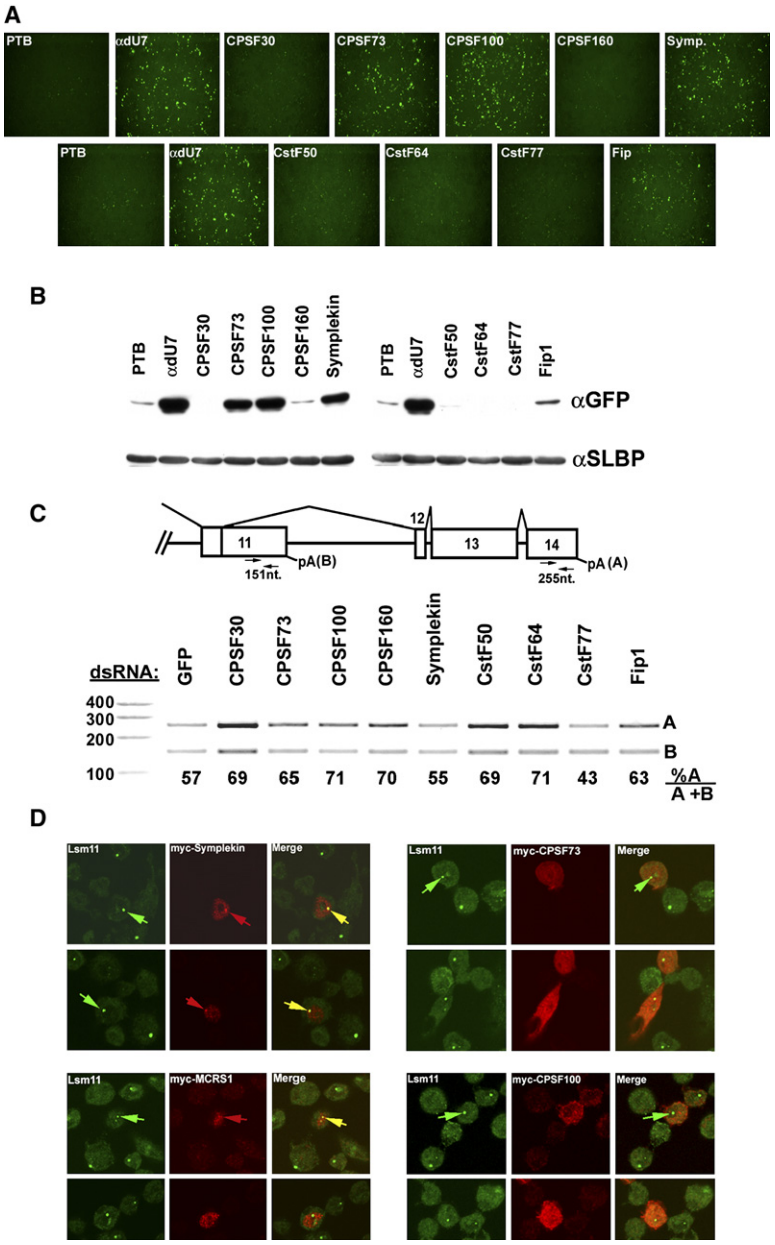

Figure 3. A Subset of Cleavage and Polyadenylation Factors Are Required for Histone Pre-mRNA Processing

(A) Fluorescence images of Dmel-2 cells treated with dsRNA targeting the indicated genes and then transfected with reporter.

(B) Western blot analysis of lysates from cells in (A).

(C) Top, schematic of the 3′ end of the *Drosophila domino* gene containing two alternative polyadenylation sites. Bottom, RT-PCR analysis of *domino* mRNA after treatment of Dmel-2 cells with the indicated dsRNAs. Band A corresponds to use of the distal poly(A) site and band B to the proximal poly(A) site. PCR products were cloned to confirm identity, and in all cases there were no products in the absence of RT.

(D) Confocal images of Dmel-2 cells transiently transfected with genes expressing the indicated myc-tagged proteins and stained with anti-Lsm11 (green) and anti-myc (red) antibodies. In merged images, yellow arrows indicate colocalization of a myc-tagged protein with Lsm11 and green arrows indicate HLB with Lsm11 only. Note that all cells contained HLB, not all of which could be visualized in the particular focal plane shown.

transcription factors, or integrator factors required for snRNA 3′ end formation (Baillat et al., 2005), suggesting that the screen detected factors directly involved in histone pre-mRNA processing. None of these dsRNAs had a large effect on cell growth. In contrast, dsRNAs against spliceosomal Sm proteins, some of which are also components of U7 snRNP, all caused cell death, accounting for our failure to identify these proteins in the screen.

Only Four of the Polyadenylation Factors Are Required for Histone Pre-mRNA Processing In Vivo

Biochemical fractionation of histone pre-mRNA processing factors from human cells suggested many of the proteins involved in cleavage and polyadenylation might be involved in histone pre-mRNA processing (Kolev and Steitz, 2005). Only four of these nine factors (CPSF73, CPSF100, Symplekin, and Fip1) scored in our screen. CPSF73 (Dominski et al., 2005) and Symplekin (Kolev and Steitz, 2005) were previously identified as histone pre-mRNA processing factors, and CPSF100 interacts with CPSF73. We depleted nine known factors involved in cleavage/polyadenylation, and only the same four factors activated the reporter (Figures 3A and 3B). All of the dsRNA-treated cells grew at near normal rates, suggesting that polyadenylation factors are present in excess in Dmel-2 cells. Indeed, the reporter requires polyadenylation to score positively. Each dsRNA treatment resulted in reduced levels of the targeted mRNA, but not of a control

mRNA (Figure S5). To determine whether the dsRNA treatment for each of the polyadenylation factors caused a functional reduction in polyadenylation, we tested the usage of polyadenylation sites in *domino* mRNA, which has short and long isoforms resulting from utilization of two different polyadenylation sites within distinct 3′ terminal exons (Ruhf et al., 2001). Depletion of seven of the nine polyadenylation factors we tested resulted in increased usage of the distal *domino* polyadenylation site (Figure 3C), whereas depletion of factors involved in histone pre-mRNA processing had no effect (Figure S6). Depletion of CPSF30, CstF64, or CstF50 resulted in the greatest usage of the distal polyadenylation site, although there was no effect on histone pre-mRNA processing. In contrast, knockdown of Symplekin scored strongly for histone pre-mRNA processing but did not affect polyadenylation of *domino* mRNA. We conclude that only a subset of cleavage/polyadenylation factors are necessary for histone pre-mRNA processing in *Drosophila* cultured cells.

Symplekin Is Concentrated in the Histone Locus Body

A nuclear structure termed the histone locus body (HLB) is associated with the *Drosophila* histone gene cluster (Liu et al., 2006). The HLB is distinct from the *Drosophila* Cajal body, which contains SMN and the U85 snRNA (Liu et al., 2006). U7 snRNP is enriched in the HLB and is visualized with antibodies against Lsm11 (Figure 3D). Other components of the HLB are likely involved in histone mRNA biosynthesis. We transiently or stably expressed Myc-tagged versions of the proteins identified in the screen and analyzed their localization with anti-Myc antibodies. Most of these proteins localized to the nucleus but did not concentrate in subnuclear foci (Table S1). An exception was Myc-tagged Symplekin, which concentrated in the HLB (Figure 3D). Myc-MCRS1 was detected in several nuclear foci, one of which often overlapped with the HLB (Figure 3D). In HeLa cells, the MCRS1 ortholog localizes to several discrete nuclear foci (Davidovic et al., 2006), some of which are coincident with Cajal bodies (E.J.W. and W.F.M., unpublished data). Myc-tagged CPSF100 and CPSF73 did not specifically concentrate in the HLB. All known mammalian U7 snRNP proteins (Lsm10, Lsm11, and ZFP100) localize to Cajal bodies. The failure to find additional proteins in the HLB other than Symplekin, Lsm10, and Lsm11 suggests that we did not identify any U7 snRNP-specific proteins.

Depletion of the Histone Variant H2Av Prevents Localization of U7 snRNP to the HLB and Histone Pre-mRNA Processing

Our screen unexpectedly identified the variant histone proteins H3.3 and H2Av, which are expressed from polyadenylated mRNAs whose synthesis is not replication coupled. H3.3 is assembled into chromatin preferentially at active genes and can be incorporated in the absence of DNA replication (Ahmad and Henikoff, 2002). *Drosophila* H2Av is a functional ortholog of both human H2A.X and H2A.Z and plays an important role in defining the boundary between euchromatin and heterochromatin and in the DNA damage response (Swaminathan et al., 2005). H2Av is present throughout the genome, including at the histone locus (Swaminathan et al., 2005; H.R.S. and R.J.D., unpublished data). The role of H2Av in histone pre-mRNA processing was confirmed in vivo by transgenic reporter gene expression in *H2Av* null mutant larvae (Figure S7). Northern blot analysis demonstrated read-through of both endogenous histone H3 and H2A mRNA (Figure 4A). Loss of H2Av expression might cause misprocessing of histone pre-mRNAs because of increased histone gene transcription, which itself might reduce processing efficiency. This is unlikely as the RNAi-mediated depletion of H2Av also results in misprocessing of a strong actin promoter-driven reporter construct (Figure S8).

To determine how H2Av contributes to histone pre-mRNA processing, we assessed the localization and activity of processing factors in H2Av-depleted cells. In wild-type salivary gland nuclei, Lsm11 antibodies detect the HLB as a prominent focus adjacent to the chromocenter, visualized by HP1 staining (Figure 4B). In contrast, there was no detectable Lsm11 focus in *H2Av* mutant salivary gland nuclei (Figure 4B). To determine whether the HLB had assembled, Mpm-2 monoclonal antibodies, which stain a phosphoprotein present in the HLB during S phase (White et al., 2007), were used to analyze both brains from *H2Av* mutant larvae (Figure 4C) and cultured cells with H2Av knocked down (Figure 4D). All cells in the wild-type larval brain contained an HLB stained by Lsm11, which colocalized with Mpm-2 staining in cells positive for Mpm-2. In contrast, many cells in *H2Av* mutant larval brains contained foci stained by Mpm-2 and lacked foci stained by Lsm11 (Figure 4C, bottom). Similarly, numerous H2Av-depeleted Dmel-2 cells contained Mpm-2 foci but not Lsm11 foci (Figure 4D). Thus, H2Av depletion results in a loss of Lsm11 from the HLB.

Western blot analysis of lysates from H2Av dsRNA-treated cells demonstrated that, in addition to a reduction in H2Av protein levels, there was also a slight decrease in the level of Lsm11 protein (Figure 4E, top three panels). There is a similar reduction in the level of U7 snRNA (Figure 4E, bottom panel). The Lsm11 mRNA levels were unchanged in H2Av-depleted cells relative to a control mRNA (Figure 4E, lower panels). Therefore, the misprocessing seen in *H2AV* null flies could result from either mislocalization of the processing machinery or from reduced levels of U7 snRNP. To address this question, we prepared nuclear extracts from control cells (PTB dsRNA), and cells treated with H2Av, Lsm11, or SLBP dsRNA, and asked whether they were competent to process a synthetic histone pre-mRNA substrate. We analyzed processing after a 1 hr incubation of a labeled histone pre-mRNA substrate in equal amounts of the various nuclear extracts (Figure 4F). Depleting Lsm11 or SLBP greatly reduced processing (Figure 4F). Mixing the extracts from Lsm11- and SLBP-depleted cells restored activity (Figure 4F, lane 5), indicating that the knockdown removed only the expected

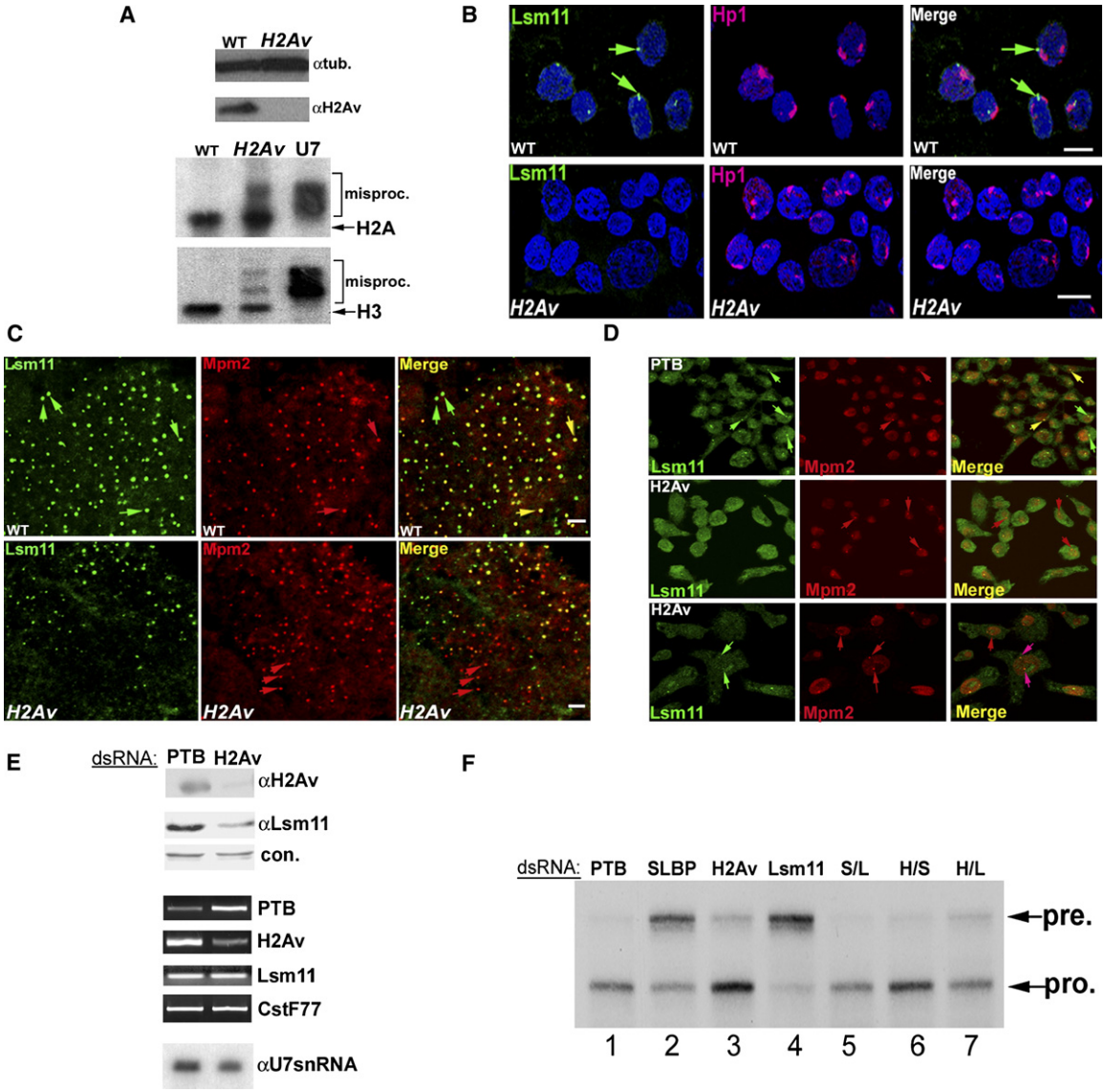

Figure 4. Knockdown of Histone Variants Affects Canonical Histone Pre-mRNA Processing

(A) Top, western blot of H2Av from wild-type and *H2Av* mutant third instar larvae. Bottom, northern blot of endogenous H2A mRNA (upper) and H3 mRNA (lower) from wild-type, *H2Av* null, and *U7* snRNA null mutant whole third instar larvae.

(B) Confocal images of salivary gland nuclei isolated from either wild-type or *H2Av* null third instar larvae stained for DNA (DAPI, blue), Lsm11 (green), and HP1 (pink). Scale bar, 20 μM.

(C and D) Confocal images of a region of a third instar larval brain from wild-type or *H2Av* mutant (C) and Dmel-2 cells treated with control dsRNA (PTB) or with H2Av dsRNA (D) stained for Lsm11 (green) and Mpm2 (red). In the merged field, green arrows indicate HLB positive for Lsm11 and negative for Mpm-2 (cells not in S phase), yellow arrows indicate HLB containing both Lsm11 and Mpm-2 (cells in S phase), pink arrows indicate HLB with Mpm-2 and reduced levels of Lsm11, and red arrows indicate HLB in H2Av-depleted cells that only contain Mpm-2. Scale bar in (C), 5 μM. Bottom panels in (D) are a higher magnification view of a different H2Av field.

(E) Dmel-2 cells treated with PTB dsRNA or H2Av dsRNA were analyzed by western blot analysis for H2Av and Lsm11 protein (top three panels). con. refers to a crossreacting band on the blot that was used as a control. RNA prepared from the same cells served as a template for RT-PCR analysis for the indicated endogenous mRNAs (next four panels). Note that the CstF77 RT-PCR serves as the loading control for all of the RT-PCRs shown. The bottom panel is a northern blot analysis of U7 snRNA in the same RNAs used in the RT-PCR analysis.

(F) In vitro processing of a labeled histone pre-mRNA incubated in nuclear extracts isolated from Dmel-2 cells treated with the indicated dsRNA. S/L, H/S, and H/L indicate processing reactions in a 1:1 mixture of nuclear extract from SLBP-, Lsm11-, or H2Av-depleted cells (S, L, H, respectively).

component required for processing. Strikingly, extracts from cells with H2Av knocked down had the same activity as control extracts (Figure 4F, lane 1 versus lane 3) and could rescue processing when mixed 1:1 with either SLBP- or Lsm11-depleted extracts (lanes 6 and 7). The failure to accumulate U7 snRNP at the HLB resulted in

a slight decrease in the overall level of U7 snRNP that was not sufficient to reduce the processing activity in H2Av-depleted cells. More importantly, these data suggest that the defect in processing in *H2Av* mutants in vivo is a result of a failure to localize U7 snRNP to the HLB, and not a defect in any processing factor.

Conclusions

Here we present in vivo evidence that a subset of proteins involved in mRNA polyadenylation are also involved in the production of histone mRNAs, which are not polyadenylated, thus demonstrating a remarkable conservation in the machinery needed to generate different mRNA 3′ ends in animal cells. We postulate that the histone pre-mRNA cleavage factor contains CPSF73/CPSF100, Symplekin, and Fip1 and other polypeptides that may be among the uncharacterized proteins identified in the screen. Of these, only Symplekin may concentrate in the HLB, consistent with its proposed role in organizing the active cleavage factor (Kolev and Steitz, 2005).

Because we did not identify known factors in snRNA or snRNP biosynthesis, many of the proteins identified in our screen are likely directly involved in histone pre-mRNA processing. In addition, we identified factors that may regulate histone pre-mRNA processing, such as Cdk2, or serve to couple transcription and processing in vivo, such as NELF-E, recently shown to be required for efficient histone pre-mRNA processing in mammalian cells (Narita et al., 2007), and H2Av, necessary for concentration of the U7 snRNP in the HLB.

This latter result suggests that cells balance assembly of variant and canonical histones by regulating pre-mRNA processing of the canonical histones. Cells deficient in H2Av do not assemble the HLB properly, and the U7 snRNP particle is not concentrated in the HLB, although it is active. The failure to properly localize the U7 snRNP to the HLB results in inefficient processing of the histone mRNA in vivo. We are currently investigating whether the failure to localize U7 snRNP is due to a specific defect in the amount of H2Av at the histone locus, or to a general H2Av deficiency.

EXPERIMENTAL PROCEDURES

Cloning of GFP Reporter

The *Drosophila* H3 promoter (see Figure 1B and Figure S1) and the first 62 amino acids of the H3 ORF were fused to the 3′UTR of histone H3, including the HDE but not the downstream polyadenylation signals. This was fused to GFP followed by the poly(A) site from the insect OpIE2 gene that was in the vector. Details of the construction of the reporter are provided in the legend to Figure S1.

Construction of Transgenic *Drosophila* Expressing the Histone/GFP Reporter

The GFP reporter was subcloned into pCaSpeR-4 to generate transgenic *Drosophila*. Brains dissected from wandering third instar larvae of the genotype w^{1118}; P [GFP reporter]/P [GFP reporter]; $U7^{EY11305}$/$U7^{EY11305}$ or w^{1118}; P [GFP reporter]/P [GFP reporter]; $Slbp^{15}$ / $Slbp^{15}$ were fixed for 20 min in 4% formaldehyde/PBS, incubated with 1° antibodies rabbit α-GFP (1:1000; Upstate) and mouse α-phosphotyrosine (1:500; Abcam) followed by 2° antibodies goat α-rabbit-Cy2 (1:500; Abcam) and goat α-mouse-Cy3 (1:500; Abcam), mounted in fluoromount-G (Southern Biotech), and analyzed with a Zeiss 510 laser scanning confocal microscope.

Cell Culture and Transfection

Dmel-2 cells (Invitrogen) were grown in serum-free conditions in SF900II-SFM media (Invitrogen). For RNA interference in 384-well plates, 8000 cells were plated in each well in 10 μl of serum-free media and incubated with 250 ng of dsRNA resuspended in 5 μl of water. Cells were allowed to grow unperturbed for 72 hr. On the third day, 20 μl of serum-free media was added to each well. Transfections were performed using Effectene reagent (QIAGEN, Valencia, CA) with a master mix using the following conditions per well: 50 ng of GFP reporter was incubated in 50 μl of EC reagent at RT for 5 min. Enhancer reagent (0.2 μl) was added to the DNA and incubated at RT for 5 min. Effectene reagent (0.3 μl) was added to the mixture and incubated for 10 min at RT. Fifty microliters of the mixture was pipetted into each well containing cells growing in 35 μl of serum-free media. For hit validation, the RNA interference was done identically, with the exception that cells were supplemented with an additional 500 ng of dsRNA 12 hr posttransfection and hence received two doses of dsRNA. For 6-well transfections, 2×10^6 cells were plated in 2 ml of serum-free media, followed by addition of 10 μg of dsRNA. Each of the following 2 days an additional 10 μg of dsRNA was added. The next day cells were transfected with 400 ng of reporter using the manufacturer's protocols.

Genome-wide RNA Interference

The screen was performed at the *Drosophila* RNAi Screening Center (DRSC) at Harvard University. Two hundred and fifty nanograms of each dsRNA included in the library are prealiquotted into 384-well, black-walled, clear-bottom plates at a concentration of 50 ng/ul. The library of 22,000 dsRNAs was distributed into a total of 63 384-well plates, and each plate had an empty well in grid position B1 in which the 2′-OCH_3 oligonucleotide to *Drosophila* U7 snRNA was added as a positive control. In grid position B2 of each plate there is a dsRNA against *thread* that kills the Dml-2 cells to control for the effectiveness of the RNAi.

The screen was performed as follows: on day 0, 8000 Dmel-2 cells in a total of 10 μl of *Drosophila* SFM-II media (GIBCO/Invitrogen) plus antibiotic/antimycotic solution (1×) were plated into each well using a Wellmate microplate dispenser (Matrix Technologies; Hudson, NH). After plating, the cells were incubated in a 24°C humidified incubator (Percival; Perry, IA). On day 3, 20 μl of SFM-II media was added to the cells, followed by transfection of the reporter construct into the cells according to the transfection protocol outline above using the microplate dispenser. Following transfection, the cells were incubated at 24°C for 2 more days. They were imaged using the Discovery-1 high content screen system (Molecular Devices; Sunnyvale, CA) equipped with a CataLyst Express (Thermo) robotic arm. Each plate was imaged using a 4× objective lens using an FITC filter set (ex. 470 nm). Using the Metamorph software suite (Molecular Devices) included with the imaging system, the images from each plate were combined into a 384 image collage and converted into fluorescence intensity plots using the software within the Metamorph program.

We compared the fluorescence signal in each well visually to that of surrounding wells and to the well containing the U7 2′-OCH_3 oligonucleotide. Positive hits were independently scored by two people (E.J.W. and B.D.B.). Our compiled lists were combined and each hit subsequently scored on a scale from 1–3, with 1 being a weak hit, 2 a moderate hit, and 3 a strong hit. To validate the hits, we synthesized templates and dsRNAs to 90 hits and used these dsRNAs in repeated RNA interference/reporter transfection experiments (n > 6). dsRNAs reproducibly resulting in increased fluorescence were included in the final list. Original collage images are available upon request.

Nuclear Extracts from RNAi-Treated Cells

Dmel-2 cells (10^7) were plated in 10 ml of SFII-900M media and incubated with 100 μg of dsRNA. The same amount of dsRNA was added to the culture each day for 2 more days. The cells were allowed to grow for 2 more days and then were harvested. Nuclear extracts were prepared as described previously (Dominski et al., 2002), with the exception that the cells were lysed in buffer A using 40 strokes through a 27.5 gauge needle. Lysates were dialyzed overnight in buffer D using a slide-a-lyzer cassette (Pierce). Processing reactions were done using 12.5 μg of nuclear extract and in conditions described previously (Dominski et al., 2002).

Supplemental Data

Supplemental Data include eight figures, one table, and Supplemental Experimental Procedures and can be found with this article online at http://www.molecule.org/cgi/content/full/28/4/692/DC1/.

ACKNOWLEDGMENTS

This research was supported by 5F32GM070101 (E.J.W.), NIH grant GM27789 (W.F.M.), and NSF grant MCB-0342847 (R.J.D.). We thank Brent Graveley for helpful discussions regarding poly(A) site selection in *Drosophila*. We thank the DRSC, especially Nadire Ramadan, for use of their facility, which is supported by GM067761 and GM067761-01S1 from the NIH.

Received: March 28, 2007
Revised: July 18, 2007
Accepted: October 3, 2007
Published: November 29, 2007

REFERENCES

Ahmad, K., and Henikoff, S. (2002). The histone variant H3.3 marks active chromatin by replication-independent nucleosome assembly. Mol. Cell *9*, 1191–1200.

Azzouz, T.N., and Schumperli, D. (2003). Evolutionary conservation of the U7 small nuclear ribonucleoprotein in Drosophila melanogaster. RNA *9*, 1532–1541.

Baillat, D., Hakimi, M.A., Naar, A.M., Shilatifard, A., Cooch, N., and Shiekhattar, R. (2005). Integrator, a multiprotein mediator of small nuclear RNA processing, associates with the C-terminal repeat of RNA polymerase II. Cell *123*, 265–276.

Boutros, M., Kiger, A.A., Armknecht, S., Kerr, K., Hild, M., Koch, B., Haas, S.A., Paro, R., and Perrimon, N. (2004). Genome-wide RNAi analysis of growth and viability in Drosophila cells. Science *303*, 832–835.

Cramer, P., Srebrow, A., Kadener, S., Werbajh, S., de la Mata, M., Melen, G., Nogues, G., and Kornblihtt, A.R. (2001). Coordination between transcription and pre-mRNA processing. FEBS Lett. *498*, 179–182.

Davidovic, L., Bechara, E., Gravel, M., Jaglin, X.H., Tremblay, S., Sik, A., Bardoni, B., and Khandjian, E.W. (2006). The nuclear microspherule protein 58 is a novel RNA-binding protein that interacts with fragile X mental retardation protein in polyribosomal mRNPs from neurons. Hum. Mol. Genet. *15*, 1525–1538.

Dominski, Z., Erkmann, J.A., Yang, X., Sanchez, R., and Marzluff, W.F. (2002). A novel zinc finger protein is associated with U7 snRNP and interacts with the stem-loop binding protein in the histone pre-mRNP to stimulate 3′-end processing. Genes Dev. *16*, 58–71.

Dominski, Z., Yang, X.C., and Marzluff, W.F. (2005). The polyadenylation factor CPSF-73 is involved in histone-pre-mRNA processing. Cell *123*, 37–48.

Godfrey, A.C., Kupsco, J.M., Burch, B.D., Zimmerman, R.M., Dominski, Z., Marzluff, W.F., and Duronio, R.J. (2006). U7 snRNA mutations in Drosophila block histone pre-mRNA processing and disrupt oogenesis. RNA *12*, 396–409.

Huang, Y., Gattoni, R., Stevenin, J., and Steitz, J.A. (2003). SR splicing factors serve as adapter proteins for TAP-dependent mRNA export. Mol. Cell *11*, 837–843.

Knoblich, J.A., Sauer, K., Jones, L., Richardson, H., Saint, R., and Lehner, C.F. (1994). Cyclin E controls S phase progression and its down-regulation during Drosophila embryogenesis is required for the arrest of cell proliferation. Cell *77*, 107–120.

Kolev, N.G., and Steitz, J.A. (2005). Symplekin and multiple other polyadenylation factors participate in 3′-end maturation of histone mRNAs. Genes Dev. *19*, 2583–2592.

Lanzotti, D.J., Kaygun, H., Yang, X., Duronio, R.J., and Marzluff, W.F. (2002). Developmental control of histone mRNA and dSLBP synthesis during Drosophila embryogenesis and the role of dSLBP in histone mRNA 3′ end processing in vivo. Mol. Cell. Biol. *22*, 2267–2282.

Liu, J.L., Murphy, C., Buszczak, M., Clatterbuck, S., Goodman, R., and Gall, J.G. (2006). The Drosophila melanogaster Cajal body. J. Cell Biol. *172*, 875–884.

Mowry, K.L., and Steitz, J.A. (1987). Identification of the human U7 snRNP as one of several factors involved in the 3′ end maturation of histone premessenger RNA's. Science *238*, 1682–1687.

Narita, T., Yung, T.M., Yamamoto, J., Tsuboi, Y., Tanabe, H., Tanaka, K., Yamaguchi, Y., and Handa, H. (2007). NELF interacts with CBC and participates in 3′ end processing of replication-dependent histone mRNAs. Mol. Cell *26*, 349–365.

Pillai, R.S., Will, C.L., Luhrmann, R., Schumperli, D., and Muller, B. (2001). Purified U7 snRNPs lack the Sm proteins D1 and D2 but contain Lsm10, a new 14 kDa Sm D1-like protein. EMBO J. *20*, 5470–5479.

Pillai, R.S., Grimmler, M., Meister, G., Will, C.L., Luhrmann, R., Fischer, U., and Schumperli, D. (2003). Unique Sm core structure of U7 snRNPs: assembly by a specialized SMN complex and the role of a new component, Lsm11, in histone RNA processing. Genes Dev. *17*, 2321–2333.

Ruhf, M.L., Braun, A., Papoulas, O., Tamkun, J.W., Randsholt, N., and Meister, M. (2001). The domino gene of Drosophila encodes novel members of the SWI2/SNF2 family of DNA-dependent ATPases, which contribute to the silencing of homeotic genes. Development *128*, 1429–1441.

Sullivan, E., Santiago, C., Parker, E.D., Dominski, Z., Yang, X., Lanzotti, D.J., Ingledue, T.C., Marzluff, W.F., and Duronio, R.J. (2001). Drosophila stem loop binding protein coordinates accumulation of mature histone mRNA with cell cycle progression. Genes Dev. *15*, 173–187.

Swaminathan, J., Baxter, E.M., and Corces, V.G. (2005). The role of histone H2Av variant replacement and histone H4 acetylation in the establishment of Drosophila heterochromatin. Genes Dev. *19*, 65–76.

Wang, Z.F., Whitfield, M.L., Ingledue, T.C., III, Dominski, Z., and Marzluff, W.F. (1996). The protein that binds the 3′ end of histone mRNA: a novel RNA-binding protein required for histone pre-mRNA processing. Genes Dev. *10*, 3028–3040.

White, A.E., Leslie, M.E., Calvi, B.R., Marzluff, W.F., and Duronio, R.J. (2007). Developmental and cell cycle regulation of the Drosophila histone locus body. Mol. Biol. Cell *18*, 2491–2502.

Wu, C.H., Lee, C., Fan, R., Smith, M.J., Yamaguchi, Y., Handa, H., and Gilmour, D.S. (2005). Molecular characterization of Drosophila NELF. Nucleic Acids Res. *33*, 1269–1279.